Pergamon

Geochimica et Cosmochimica Acta, Vol. 61, No. 15, pp. 3161–3169, 1997

0016-7037/97 $17.00 + .00

PII S0016-7037(97)00135-X

# The boron isotope geochemistry of the neogene borate deposits of western Turkey

M. R. PALMER[1] and C. HELVACI[2]

[1]Department of Geology, University of Bristol, Bristol, BS8 1RJ, England
[2]Dokuz Eylül Üniversitesi, Mühendislik Fakültesi, Jeoloji Mühendisligi Bölümü, 35100 Bornova-Izmir, Turkey

(*Received November* 11, 1996; *accepted in revised form March* 17, 1997)

**Abstract**—We have analyzed the boron isotope composition of 80 borate minerals (major minerals: borax, colemanite, and ulexite; minor minerals: veatchite-A, tunellite, kernite, terrugite, probertite, meyerhofferite, inderite, inyoite, hydroboracite, howlite, and pandermite) from the main deposits (Kirka, Bigadiç, and Emet) and two smaller deposits (Kestelek and Sultançayir) in the western Turkish borate deposits. Forty-three samples were also analysed for their Sr isotope composition. The data span a wide range in $\delta^{11}B$ values from −1.6‰ to −25.3‰. The $\delta^{11}B$ values of the main borate minerals are largely controlled by their mineralogy and the pH of the brines from which they precipitated. An inverse correlation between the average $\delta^{11}B$ and $^{87}Sr/^{86}Sr$ ratios of colemanite in the different deposits suggests there is some variation in the sources of boron and Sr to the deposits. Emet has the highest contribution from aluminosilicates and Kirka the highest contribution from Eocene carbonates, with Bigadiç occupying an intermediate position. The $\delta^{11}B$ values of the minor borate minerals distinguish between those which are primary precipitates from the original brines (or formed from primary borates without boron loss from the system) and those which formed from alteration of preexisting borate minerals with substantial loss of boron from the system. 

## 1. INTRODUCTION

Nonmarine evaporite deposits play an important role in the geologic record, e.g., they record paleoclimatic conditions, they form in specific tectonic environments, they can aid in the formation of major metal ore deposits, and they can form ore bodies in themselves (Palmer and Slack, 1989; Slack et al., 1989; Smoot and Lowenstein, 1991; Peng and Palmer, 1995). Borate-bearing nonmarine evaporites are the largest industrial source of boron in the world, with the major production coming from the U.S.A. and Turkey (Kistler and Helvaci, 1994). We recently carried out a boron isotope study of borates from the Kirka borate deposit, Turkey, and demonstrated that boron isotopes reveal information concerning the physicochemical conditions under which the borates were formed (Palmer and Helvaci, 1995). Here, we compare these data with the boron isotope compositions of borates from other Neogene borate deposits in Western Turkey.

## 2. GEOLOGICAL SETTING

The Turkish borate deposits in Western Anatolia are located in five main districts: Bigadiç, Kestelek, Sultançayir, Emet, and Kirka (Fig. 1). They formed in a lacustrine environment during periods of calc-alkaline volcanic activity in the Neogene. There are differences between the different districts, but the borates are all generally enclosed within limestones and clays and are interbedded with layers of volcanic ash, limestone, marl, and clays (Inan et al., 1973; Helvaci, 1977; Sunder, 1980). The main boron minerals are borax, colemanite, and ulexite, with the proportions of these minerals varying between the deposits. A large number of other borate minerals are found in the deposits, including pandermite, inyoite, meyerhofferite, tincalconite, kernite, hydroboracite, inderite, inderborite, kurnakovite, terrugite, veatchite-A, and tunnelite (Inan et al., 1973; Helvaci, 1977, 1978, 1983). The boron in the deposits is assumed to be derived from leaching of the surrounding rocks by geothermal activity associated with local volcanism. The borates then formed when the spring waters evaporated after flowing into shallow playa lakes (Helvaci, 1995).

## 3. EXPERIMENTAL

### 3.1. Sampling

Eighty samples from the borate district were analyzed for their boron isotope compositions. Of these, 43 were also analyzed for their Sr isotope ratios. Several samples contained different generations of crystals of the same mineral (such as fillings in septarian cracks in nodules) or intergrowths of different minerals. These were separated by handpicking and analyzed as different samples. All samples were handpicked under a binocular microscope to ensure that they were free of adhering clay and were pure mineral separates. Brief sample descriptions are given in the Appendices.

### 3.2. Analytical

The boron was extracted by pyrohydrolysis at 1400°C (Spivack and Edmond, 1986). The boron isotope compositions were measured according to the method described by Aggarwal and Palmer (1994). The data are reported as $\delta^{11}B$ values where

$$\delta^{11}B = \left[ \left\{ \frac{^{11}B/^{10}B_{sample}}{^{11}B/^{10}B_{standard}} \right\} - 1 \right] \times 10^3$$

The standard is NBS boric acid SRM 951. At Bristol, ~100 analyses of this standard over three years on a VG336 mass spectrometer yielded an average $^{11}B/^{10}B$ ratio of 4.0529 ± 0.1‰ (2s). The average 2s error of the 160 individual measurements in this study is ±0.32‰. Replicate analyses were made of each sample. The average agreement between these replicates is slightly poorer at ±0.50‰, and may reflect isotope heterogeneity in some samples, together with analytical artefacts.

Strontium isotope ratios were measured on a selected suite of the samples using the same mass spectrometer. The ratios were

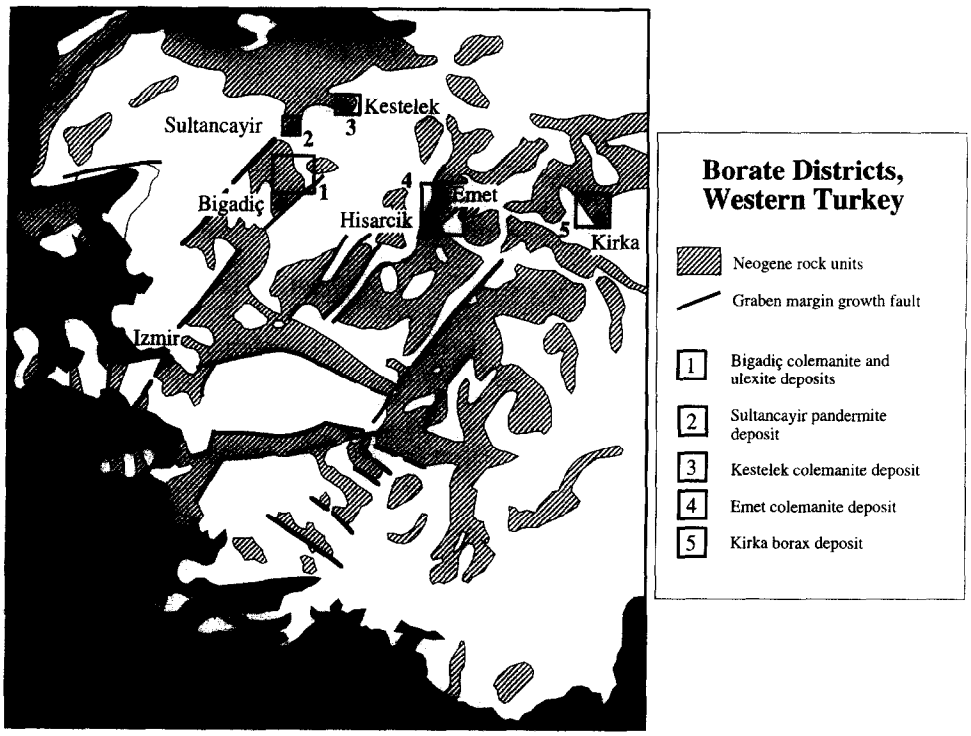


Fig. 1. Location of major borate deposits in western Turkey.

normalised to an $^{88}Sr/^{86}Sr$ ratio of 0.1194 and an $^{87}Sr/^{86}Sr$ value of 0.7080 for the E & A standard. We have obtained an average $^{87}Sr/^{86}Sr$ ratio of 0.70796 for fifteen measurements of this standard.

## 4. RESULTS

Results are listed in Tables 1–4, and the structural formulae, basic boron atomic structure (Anovitz and Hemingway, 1996), and reduced partition function ratios (RPFR) of the borate minerals considered in this study are given in Table 5. The RPFR are derived from the data presented in Oi et al. (1989). Those minerals having the highest proportion of trigonally coordinated boron have the highest RPFR. If two minerals are precipitated from identical brines under the same physical conditions, the mineral having the highest RPFR will have the heaviest (less negative) $\delta^{11}B$ values. The RPFR of Oi et al. (1989) are the products of theoretical calculations. It would be preferable to use experimentally determined isotope fractionation factors, but there are major kinetic difficulties in precipitating many borate minerals in the laboratory (e.g., Helvaci, 1977), and isotope fractionation experiments would suffer from the additional problems of maintaining constant pH and temperature conditions over the lengthy time required to form the borates. There may be discrepencies between the absolute values of the isotope fractionation factors calculated by Oi et al. (1989) and the true values, but the relative isotope fractionation factors are most likely correct, as the isotope fractionation mechanism of boron is relatively well understood (e.g., Palmer, 1996). In addition, support for the accuracy of the theoretical approach is provided by the good agreement between high temperature theoretical boron isotope fractionation factors calculated by Kakihana et al. (1977) and experimental data at similar temperatures (Palmer et al., 1992).

The data span a wide range in $\delta^{11}B$ values from −1.6‰ in a sample of borax from Kirka to −25.4‰ in a sample of terrugite from the Hisarcik mine in the Emet deposit. In contrast, the $^{87}Sr/^{86}Sr$ ratios show a relatively narrow range,

Table 1. Boron and strontium isotope compositions of borate minerals from the Kirka deposit

| Sample | Mineralogy | $\delta^{11}B$ 1st run | $\delta^{11}B$ 2nd run | $^{87}Sr/^{86}Sr$ |
|---|---|---|---|---|
| CH-5 | pandermite | -17.0±.3 | -16.5±.4 | 0.70849±14 |
| CH-7 | ulexite* | -6.2±.2 | -6.8±.4 | 0.70862±15 |
| CH-8 | borax* | -1.6±.2 | -2.7±.3 | 0.70891±30 |
| CH-9 | ulexite* | -10.1±.2 | -10.6±.3 | 0.70890±09 |
| CH-10 | ulexite* | -8.0±.3 | -7.5±.4 | 0.70855±31 |
| CH-11 | kernite | -6.5±.4 | -7.4±.4 | 0.70907±35 |
| CH-12 | ulexite* | -7.8±.3 | -7.7±.2 | 0.70830±35 |
| CH-14 | borax* | -5.7±.2 | -5.0±.2 | 0.70865±09 |
| CH-15 | borax* | -5.1±.2 | -5.7±.3 | 0.70874±06 |
| CH-16 | colemanite* | -12.9±.3 | -13.3±.2 | 0.70916±07 |
| CH-17 | colemanite* | -9.6±.3 | -9.9±.4 | 0.70861±08 |
| CH-17 | ulexite* | -7.6±.2 | -7.5±.2 | 0.70864±10 |
| CH-18 | borax* | -5.1±.4 | -4.3±.2 | 0.70943±07 |
| CH-18 | ulexite* | -7.9±.4 | -7.6±.5 | 0.70941±06 |
| CH-22 | colemanite* | -13.3±.3 | -13.4±.3 | |
| CH-24 | borax* | -1.6±.3 | -2.4±.3 | 0.70889±03 |
| CH-57 | tunellite | -4.4±.2 | -4.2±.6 | |
| MRP-4 | borax* | -3.3±.4 | -2.6±.2 | |
| MRP-5 | borax* | -3.3±.2 | -4.1±.3 | |
| MRP-11 | 1°ulexite* | -5.7±.4 | -6.4±.5 | |
| MRP-11 | ulexite in cracks* | -5.9±.4 | -5.3±.4 | |
| MRP-12 | 1° colemanite* | -12.8±.6 | -12.4±.5 | |
| MRP-12 | colemanite in cracks* | -11.4±.3 | -11.3±.4 | |
| MRP-12 | 2° colemanite* | -14.9±.5 | -14.7±.3 | |
| MRP-14 | central colemanite* | -14.7±.4 | -14.7±.4 | |
| MRP-14 | outer colemanite* | -13.7±.2 | -13.7±.3 | |
| MRP-17 | ulexite* | -6.7±.3 | -6.0±.2 | |

* Data from Palmer and Helvaci (1995)

Table 2. Boron and strontium isotope compositions of borate minerals from the Bigadiç deposit

| Sample | Mineralogy | $\delta^{11}B$ 1st run | $\delta^{11}B$ 2nd run | $^{87}Sr/^{86}Sr$ |
|---|---|---|---|---|
| Simav | | | | |
| CH-1 | colemanite | -16.3±.2 | -15.7±.4 | 0.70794±13 |
| CH-2 | pandermite | -16.7±.4 | -16.0±.4 | 0.70735±07 |
| CH-25 | colemanite | -8.3±.3 | -7.4±.3 | 0.70773±19 |
| CH-25 | ulexite | -6.4±.3 | -6.1±.3 | 0.70802±16 |
| CH-43 | colemanite | -9.6±.3 | -10.1±.3 | 0.70838±14 |
| CH-49 | colemanite | -9.9±.3 | -10.7±.3 | 0.70822±33 |
| CH-52 | meyerhofferite | -9.3±.4 | -9.5±.3 | 0.70795±10 |
| CH-53 | ulexite | -4.9±.2 | -5.5±.4 | 0.70835±18 |
| MRP-44 | meyerhofferite | -10.5±.2 | -11.4±.5 | |
| MRP-44 | colemanite | -10.3±.3 | -10.2±.4 | |
| MRP-48 | colemanite | -9.9±.4 | -9.7±.3 | |
| Acep | | | | |
| CH-13 | colemanite | -9.6±.2 | -9.6±.2 | 0.70820±18 |
| CH-21 | inyoite | -8.6±.3 | -7.9±.4 | 0.70851±09 |
| MRP-40 | 1° colemanite | -9.4±.4 | -8.9±.3 | |
| MRP-40 | 2° colemanite | -12.7±.5 | -12.5±.4 | |
| MRP-47 | inyoite | -10.0±.3 | -9.4±.4 | |
| MRP-47 | colemanite | -12.0±.2 | -12.4±.5 | |
| MRP-47 | ulexite | -8.8±.2 | -9.2±.3 | |
| Kireçlik | | | | |
| CH-44 | colemanite | -11.3±.3 | -10.8±.3 | 0.70803±22 |
| CH-51 | colemanite | -12.2±.4 | -13.0±.2 | |
| CH-54 | ulexite | -6.2±.3 | -5.6±.4 | 0.70786±23 |
| Kurtpinari | | | | |
| CH-3 | ulexite | -9.6±.4 | -8.6±.6 | 0.70816±24 |
| CH-46 | colemanite | -11.7±.4 | -10.9±.4 | 0.70815±08 |
| CH-50 | howlite | -13.5±.3 | -13.7±.4 | |
| On Günevi | | | | |
| CH-45 | ulexite | -5.3±.1 | -4.9±.2 | 0.70874±06 |
| Tülü | | | | |
| CH-4 | colemanite | -12.0±.3 | -11.0±.3 | 0.70835±05 |
| CH-47 | colemanite | -12.2±.4 | -11.5±.4 | 0.70802±13 |
| CH-48 | colemanite | -5.6±.3 | -4.6±.3 | |
| MRP-34 | 1° colemanite | -8.6±.3 | -7.9±.2 | |
| MRP-34 | 2° colemanite | -14.4±.4 | -15.1±.4 | |
| MRP-36 | pandermite | -12.8±.3 | -12.8±.4 | |

from 0.70962 in a sample of colemanite from the Killik mine in the Emet deposit to 0.70735 in a sample of pandermite from the Simav mine in the Bigadiç deposit. The average Rb/Sr ratio of the borate minerals is only $4.3 \times 10^{-3}$ and the half-life of $^{87}Rb$ is too long for there to have been any significant change in the $^{87}Sr/^{86}Sr$ ratio of the borates in the $\sim 20 \times 10^6$ years since their formation.

## 5. DISCUSSION

The boron isotope composition of a borate mineral is a function of the $\delta^{11}B$ value of the source of boron, its RPFR, the temperature of formation of the borate, the pH of the solution during precipitation of the borate, and the proportion of borates precipitated from the brines (Rayleigh effects) (Palmer and Helvaci, 1995).

Table 3. Boron and strontium isotope compositions of borate minerals from the Kestelek and Sultançayri deposits

| Sample | Mineralogy | $\delta^{11}B$ 1st run | $\delta^{11}B$ 2nd run | $^{87}Sr/^{86}Sr$ |
|---|---|---|---|---|
| Kestelek | | | | |
| CH-19 | colemanite | -15.9±.2 | -15.7±.2 | |
| CH-36 | colemanite | -25.3±.2 | -25.3±.4 | 0.70862±15 |
| CH-37 | ulexite | -9.2±.2 | -10.2±.2 | 0.70841±13 |
| CH-38 | probertite | -12.4±.2 | -12.5±.3 | 0.70831±16 |
| CH-39 | hydroboracite | -9.5±.4 | -10.5±.4 | |
| Sultançayir | | | | |
| CH-20 | pandermite | -24.5±.2 | -23.8±.2 | 0.70861±08 |
| CH-90 | pandermite | -16.3±.4 | -16.0±.3 | |
| | colemanite | -11.1±.4 | -11.1±.5 | |
| CH-91 | howlite | -23.0±.4 | -22.4±.4 | |
| CH-92 | howlite | -26.3±.4 | -26.1±.4 | |

Table 4. Boron and strontium isotope compositions of borate minerals from the Emet deposits

| Sample | Mineralogy | $\delta^{11}B$ 1st run | $\delta^{11}B$ 2nd run | $^{87}Sr/^{86}Sr$ |
|---|---|---|---|---|
| Killik | | | | |
| CH-23 | colemanite | -12.1±.3 | -12.4±.5 | 0.70962±04 |
| CH-27 | hydroboracite | -13.2±.3 | -13.4±.4 | 0.70875±06 |
| CH-28 | veatchite-A | -8.5±.4 | -9.4±.4 | 0.70948±15 |
| Espey | | | | |
| CH-26 | 1° colemanite | -14.6±.3 | -14.4±.3 | |
| CH-26 | 2° colemanite | -16.3±.4 | -16.9±.4 | |
| CH-32 | hydroboracite | -12.1±.4 | -12.6±.4 | 0.70826±05 |
| MRP-18 | colemanite | -13.2±.4 | -13.4±.4 | |
| MRP-21 | 1° colemanite | -14.8±.3 | -15.1±.3 | |
| MRP-21 | 2° colemanite | -16.3±.2 | -15.5±.4 | |
| MRP-23 | hydroboracite | -11.9±.3 | -12.5±.3 | |
| Göktepe | | | | |
| CH-33 | colemanite | -15.4±.1 | -15.2±.3 | |
| Dereköy | | | | |
| CH-30 | colemanite | -15.4±.2 | -16.4±.2 | |
| Hisarcik | | | | |
| CH-6 | colemanite | -15.1±.4 | -14.9±.4 | |
| CH-29 | colemanite | -14.6±.2 | -14.7±.4 | 0.70860±20 |
| CH-34 | colemanite | -17.0±.4 | -17.7±.4 | 0.70946±06 |
| CH-42 | colemanite | -16.0±.2 | -15.7±.2 | 0.70910±06 |
| CH-56 | terrugite | -24.6±.3 | -25.4±.4 | |

### 5.1. Major Borate Minerals

Previously, we carried out a detailed study of the $\delta^{11}B$ value of the main borates (borax, ulexite, and colemanite) from Kirka (Palmer and Helvaci, 1995). This study showed there was no obvious correlation between boron and Sr isotope ratios for individual borate minerals, i.e., varying sources of boron to the deposits did not control the variations in $\delta^{11}B$ values within an individual deposit. The relative differences in the $\delta^{11}B$ values of the three borate minerals were consistent with their RFPR, but the magnitude of the differences in $\delta^{11}B$ values between the minerals was too large for them to have precipitated together from brines with the same $\delta^{11}B$ values and pH. The data were consistent with all three minerals being primary precipitates from the evaporite brine, with colemanite precipitating from a brine of lower pH than ulexite, and borax precipitating from a brine of higher pH than ulexite. The borates did not maintain boron isotope equilibrium with the coexisting brine after precipitation from solution. Rayleigh fractionation models suggest that the $\delta^{11}B$ value of the brines that formed borax were slightly heavier than those that precipitated ulexite and colemanite (Palmer and Helvaci, 1995).

These same processes likely operated to control borate $\delta^{11}B$ values throughout the western Turkish borate province. For example, minerals with higher RPFR tend to have higher $\delta^{11}B$ values in each of the deposits where they coexist (Fig. 2). However, there are differences in the geology of the deposits that may have implications for their boron isotope systematics.

The most obvious difference is the absence of significant amounts of borax in all but the Kirka deposit. In all other deposits, colemanite and ulexite are the dominant borates. This suggests that the fluids that fed the playa lake in which the Kirka deposit formed were Na-rich relative to the rest of the area. If brines from the different deposits had different

Table 5. Structural formulae, basic boron atomic structure and reduced partition function ratios (RPFR) of borate minerals analyzed in this study

| Boron Mineral | Structural Formula | Basic boron atomic structure | RPFR (25°C) |
|---|---|---|---|
| veatchite-A | $Sr_2B_{11}O_{16}(OH)_5.H_2O$ | no structure refinement known | |
| pandermite (=priceite) | $Ca_4B_{10}O_{19}7H_2O$ | no structure refinement known | |
| tunellite | $SrB_6O_9(OH)_2.3H_2O$ | $3BO_3 + 3BO_4$ | 1.1894 |
| borax | $Na_2B_4O_5(OH)_4.8H_2O$ | $2BO_3 + 2BO_4$ | 1.1894 |
| kernite | $Na_2B_4O_6.(OH)_2.3H_2O$ | $2BO_3 + 2BO_4$ | 1.1894 |
| ulexite | $NaCaB_5O_6(OH)_6.5H_2O$ | $2BO_3 + 3BO_4$ | 1.1871 |
| probertite | $NaCaB_5O_7(OH)_4.3H_2O$ | $2BO_3 + 3BO_4$ | 1.1871 |
| teruggite | $Ca_4Mg[AsB_6O_{11}(OH)_6]_2.14H_2O$ | $4BO_3 + 8BO_4$ | 1.1856 |
| colemanite | $CaB_3O_4(OH)_3.H_2O$ | $BO_3 + 2BO_4$ | 1.1856 |
| meyerhofferite | $Ca_2B_6O_6(OH)_{10}.2H_2O$ | $2BO_3 + 4BO_4$ | 1.1856 |
| inderite | $MgB_3O_3(OH)_5.5H_2O$ | $BO_3 + 2BO_4$ | 1.1856 |
| inyoite | $Ca_2B_6O_6(OH)_{10}.8H_2O$ | $2BO_3 + 4BO_4$ | 1.1856 |
| hydroboracite | $CaMg[B_3O_4(OH)_3]_2.3H_2O$ | $BO_3 + 2BO_4$ | 1.1856 |
| howlite | $Ca_2SiB_5O_9(OH)_5$ | $BO_3 + 6BO_4$ | 1.1813 |

Structural formula and basic atomic structure from Anovitz and Hemingway (1996)

chemical compositions, they may also have had different $\delta^{11}B$ values. Potential boron sources include Paleozoic metamorphics, Mesozoic ophiolites, and Eocene limestones, as well as the calc-alkaline volcanics that formed at the same time as the borates (Inan et al., 1973; Helvaci, 1977; Sunder, 1980). Boron and strontium have a common origin in several borate deposits (Bowser, 1965; Helvaci, 1984, 1995; Alonso et al., 1988), so a correlation between their isotope ratios might be expected if there had been changes in the relative contributions of B and Sr from these sources. Eocene limestones have $^{87}Sr/^{86}Sr$ ratios of ~0.7078 (DePaolo and Ingram, 1985), whereas aluminosilicate rocks generally have more radiogenic Sr isotope ratios. In contrast, limestones have higher $\delta^{11}B$ values (0 to +6‰) than aluminosilicates (−17 to −6‰) (Ishikawa and Nakamura, 1993; Palmer, 1996). A plot of $^{87}Sr/^{86}Sr$ ratios versus average $\delta^{11}B$ values of primary colemanite in the Emet, Kirka, and Bigadiç deposits shows an inverse relationship, indicating variations in the proportions of Sr and B derived from limestones and silicate rocks (Fig. 3). However, there is no significant correlation between Sr and boron isotope compositions for colemanite within individual deposits. Hence, the relative contributions of B and Sr within individual deposits from silicate and carbonate rocks appear to have remained relatively constant (Palmer and Helvaci, 1995).

The differences in the $\delta^{11}B$ values of the three main borate minerals at Kirka are greater than would be expected if they had precipitated in equilibrium with one another (Palmer and Helvaci, 1995). The only other deposit in which there are significant amounts of coexisting primary borate minerals is at Bigadiç, which contains coexisting ulexite and colemanite, where the average $\delta^{11}B$ value of ulexite (−6.8‰) is 3.6‰ higher than that of colemanite (−10.4‰). This differ-

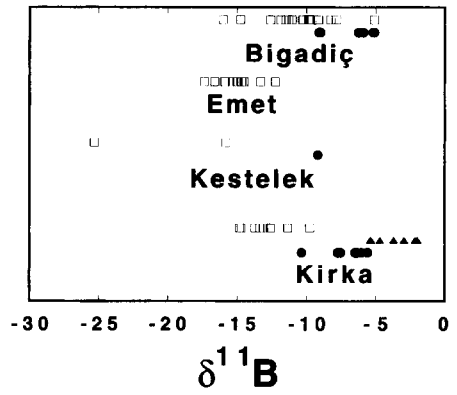


Fig. 2. Range of boron isotopes in major borate minerals (squares = colemanite, circles = ulexite, triangles = borax).

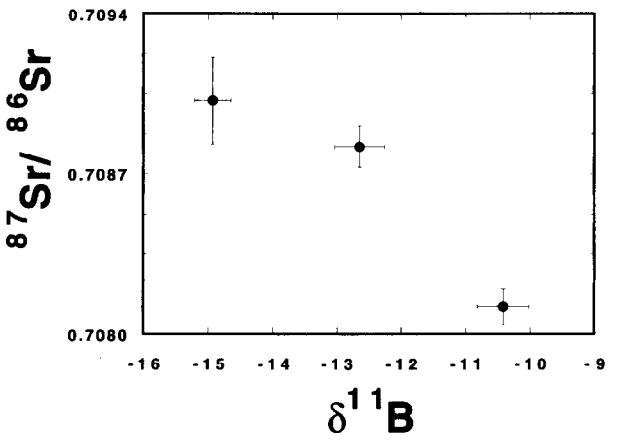


Fig. 3. Relationship between average $^{87}Sr/^{86}Sr$ ratios and $\delta^{11}B$ values in colemanite from the Bigadiç, Kirka, and Emet deposits (error bars are 1s variations of the data within the individual deposits).

ence is greater than that predicted by theoretical calculations (1.3‰) (Oi et al., 1989), suggesting that colemanite precipitated at a lower pH than ulexite (Palmer and Helvaci, 1995).

### 5.2. Minor Borate Minerals

In addition to the three main ore-forming borate minerals (borax, ulexite, and colemanite), there are a large number of less abundant borates in the Turkish deposits (e.g., Helvaci, 1994, 1995). In some cases it is uncertain whether these minerals are precipitates from the evaporite brine or alteration products of primary borate minerals.

Pandermite (= priceite), $Ca_4B_{10}O_{10} \cdot 7H_2O$, is generally thought to be a primary mineral in Turkey (Helvaci, 1994), although elsewhere it has been suggested as a hydration product of colemanite (Anovitz and Hemingway, 1996). Its formation in preference to colemanite is favoured by higher water activities and higher $Ca^{2+}/H^+$ ratios (Christ et al., 1967). Pandermite has been analyzed from the Kirka (−16.8‰), Bigadiç (−16.4‰ and −12.8‰), and Sultançayir (−24.2‰ and −16.2‰) deposits. Unfortunately, there is no structural refinement for pandermite, so it is not possible to calculate its RPFR. The $\delta^{11}B$ values of pandermite in Kirka and Bigadiç are lighter (by ~4‰) than average primary colemanite from these deposits. If this pandermite is primary, the mineral must have a lower RPFR than colemanite or have formed from a brine of different composition (i.e., different pH, temperature, or $\delta^{11}B$ value). The data preclude isochemical alteration of colemanite to pandermite. One of the two samples of pandermite from Sultançayir has a very light $\delta^{11}B$ value (−24.2‰). This sample occurs as centimetre-sized nodules in a clay-gypsum matrix, whereas the pandermite samples from the Kirka and Bigadiç deposits are massive and monominerallic. The very light $\delta^{11}B$ value of pandermite from Sultançayir suggests that the nodules are secondary products formed from the dissolution of preexisting borate minerals, coupled with substantial loss of boron from the system. The other sample of pandermite from Sultançayir is ($\delta^{11}B$ value; −16.2‰) occurs in the interstices of small radiating colemanite nodules ($\delta^{11}B$ value; −11.1‰), suggesting it either formed as a primary precipitate (as at Kirka and Bigadiç) or that there was less boron loss during transformation of colemanite to pandermite.

Kernite ($Na_2B_4O_6 \cdot (OH)_2 \cdot 3H_2O$) is restricted to the Na-rich Kirka deposit in Turkey. Its formation is favoured, with respect to borax, by a lower water activity and higher temperature. The temperature of the borax-kernite transition varies from 38 to 59°C, depending on the brine composition (Christ et al., 1967; Inan, 1973). Kernite has the same RPFR as borax, so if it is a primary mineral it should have a similar $\delta^{11}B$ value, providing there has been no loss of boron from the system. Transformation of kernite from borax occurs by

$$\underset{\text{borax}}{Na_2B_4O_5(OH)_4 \cdot 8H_2O} \rightarrow \underset{\text{kernite}}{Na_2B_4O_6(OH)_2 \cdot 3H_2O} + 6H_2O \quad (2)$$

If the water released from the breakdown of borax is concentrated along veins and expelled from the system, the high solubility of borates means that it is possible that kernite dissolution may occur in areas where the water flow is concentrated. If boron loss occurs and the pH is < ~8.8 the secondary kernite will have a lighter $\delta^{11}B$ than the primary borax,but if the pH of the aqueous solution is > ~8.8 the $\delta^{11}B$ of the kernite would be heavier (cf. Palmer and Helvaci, 1995, Fig. 3). The kernite sample analyzed from Kirka has a slightly lighter $\delta^{11}B$ value (−7‰) compared to borax from this deposit (average −3.8‰, range −1.6 to −5.7‰), suggesting that kernite formed from dehydration of borax at a pH <8.8 with some loss of boron and water from the system.

Tunellite ($SrB_6O_9(OH)_2 \cdot 3H_2O$) is a rare mineral that has been identified in several Turkish deposits (Helvaci, 1984, 1995), but only one sample ($\delta^{11}B$ = −4.3‰) from Kirka was analyzed in this study. Tunellite is thought to form by dissolution and recrystallization of Sr-rich ulexite and colemanite (Helvaci, 1995).

$$\underset{\text{primary ulexite}}{NaCaB_5O_9 \cdot 8H_2O} + SrO + 6H_3BO_3 \rightarrow \underset{\text{tunellite}}{SrB_6O_{10} \cdot 4H_2O} + \underset{\text{secondary ulexite}}{NaCaB_5O_9 \cdot 8H_2O} + 5H_2O \quad (3)$$

$$\underset{\text{primary colemanite}}{CaB_3O_4(OH)_3 \cdot H_2O} + SrO + 6H_3BO_3 \rightarrow \underset{\text{tunellite}}{SrB_6O_{10} \cdot 4H_2O} + \underset{\text{secondary colemanite}}{CaB_3O_4(OH)_3 \cdot H_2O} + 5H_2O \quad (4)$$

The tunellite sample analyzed here is from the ulexite-colemanite transition zone, but neither mineral was associated tunellite in the sample. Both reactions involve addition of boron to the system, so it is difficult to evaluate the signifcance of the tunellite boron isotope data without a knowledge of the $\delta^{11}B$ value of this additional source of boron. Tunellite has a high RPFR (Table 5), which is consistent with its relatively high $\delta^{11}B$ value compared to average colemanite (−12.7‰) and ulexite (−7.3‰) at Kirka.

The other Sr borate analyzed here is veatchite-A sample from Emet ($2Sr_2[B_5O_8(OH)]_2 \cdot B(OH)_3 \cdot H_2O$). Field and textural evidence suggest this mineral formed from alteration of colemanite (Helvaci and Firman, 1976). There is no structural refinement for veatchite-A, but comparing the relatively high $\delta^{11}B$ value of veatchite-A from this study (−8.9‰) to average colemanite (−14.9‰) from Emet suggests either that veatchite-A has a higher proportion of trigonally coordinated boron than does colemanite, or that boron with a heavier $\delta^{11}B$ value was introduced into the system during alteration. The data precludes boron conservation during the alteration of colemanite to veatchite-A in this sample.

Meyerhofferite ($CaB_3O_3(OH)_5 \cdot H_2O$) may form either directly from an evaporite brine or by dehydration of inyoite ($CaB_3O_3(OH)_5 \cdot 4H_2O$). Christ et al. (1967) considered meyerhofferite to be a metastable phase formed by the alteration of inyoite, with no evidence of reaction between colemanite and meyerhofferite. In this study, two samples of meyerhofferite were analyzed from Bigadiç (−10.9 and −9.4‰). Meyerhofferite has the same RPFR as colemanite and inyoite, and the $\delta^{11}B$ values of meyerhofferite are similar to average colemanite from Bigadiç (−10.4‰) and the two samples of inyoite from this deposit (−9.7 and −8.3‰). If meyerhofferite precipitated directly from the brine, it might be expected to have the same $\delta^{11}B$ value as coexisting cole-

manite or inyoite. However, if it formed by dehydration of inyoite, it may have a slightly lighter $\delta^{11}B$ value if boron was lost from the system with the water. In one case (sample MRP-44) meyerhofferite and colemanite are intergrown, with no evidence of replacement reactions between the two minerals. The $\delta^{11}B$ values of the colemanite and meyerhofferite are similar ($-10.3‰$ and $-10.9‰$, respectively), suggesting that both formed directly from the evaporite brine in this case. The $\delta^{11}B$ values of inyoite are only slightly heavier than the average $\delta^{11}B$ value of colemanite, and also suggest that inyoite was formed directly from the brine.

Howlite ($Ca_2SiB_5O_9(OH)_5$) is unequivocally a secondary mineral (Countryman, 1977). In the Turkish deposits textural evidence suggests howlite was formed by the alteration of colemanite by Si released from the alteration of coexisting clays and volcanic ash (Helvaci and Firman, 1976).

$$\underset{\text{colemanite}}{5CaB_3O_4(OH)_3\cdot H_2O} + 3SiO_2 + CaO \rightarrow \underset{\text{howlite}}{3Ca_2SiB_5O_9(OH)_5} + 5H_2O \quad (5)$$

Howlite has a complicated atomic structure, in which boron is present in the $[Si_2B_4O_{10}(OH)_6\cdot B_3O_4(OH)_2]^{\infty}$ polyanion (Griffen, 1988); hence the basic atomic structure of boron in howlite is $BO_3 + 6BO_4$, giving it the lowest RPFR of all the borate minerals considered here (Table 5). The extent of boron isotope fractionation between primary colemanite and the secondary howlite depends on the extent of any boron loss during the reaction, but if the two minerals were in equilibrium the howlite should have a $\delta^{11}B$ that is $3.6‰$ lighter than colemanite. The one howlite sample from Bigadiç and has a $\delta^{11}B$ of $-13.6‰$, which is within the range of $\delta^{11}B$ values shown by colemanite in this deposit, suggesting that boron was largely conserved during the alteration. In contrast, howlite from Sultançayir has the lightest $\delta^{11}B$ values measured in this study ($-22.7$ and $-26.2‰$) and indicates there was substantial loss of boron from the system during formation of howlite in this case.

Probertite ($NaCaB_5O_7(OH)_4\cdot 3H_2O$) is rare in the Turkish borate deposits. It is most likely formed by partial dehydration of ulexite, with which it shares the same basic atomic structure. The one example of probertite analyzed here is from Kestelek and has a lighter $\delta^{11}B$ value ($-12.5‰$) than ulexite ($-9.7‰$) from the same deposit, suggesting that some boron may have been lost from the system during dehydration.

Hydroboracite ($CaMg[B_3O_4(OH)_3]_2\cdot 3H_2O$) is relatively common in the Emet deposit, where it is generally intergrown with colemanite and sometimes cut by later colemanite veins. It is thought to form by exchange reactions between colemanite and Mg-rich tuffs and clays (Helvaci and Firman, 1976).

$$2\underset{\text{colemanite}}{[CaB_3O_4(OH)_3\cdot H_2O]} + Mg^{2+} + 2H_2O \rightarrow \underset{\text{hydroboracite}}{CaMg[B_3O_4(OH)_3]_2\cdot 3H_2O} + Ca^{2+} \quad (6)$$

The two minerals have identical RFPR, so no boron isotope fraction between coexisting colemanite and hydroboracite is expected if boron is conserved. The $\delta^{11}B$ values of the three hydroboracite samples from Emet ($-12.2$ to $-13.3‰$) are similar to the range ($-12.2$ to $-17.4‰$) in primary colemanite $\delta^{11}B$ values from this deposit, suggesting that boron is generally conserved during the alteration reaction.

Terruggite ($Ca_4Mg[AsB_6O_{11}(OH)_6]_2\cdot 14H_2O$) is a rare mineral that is restricted to the As- and S-rich Emet deposit amongst the Turkish borate deposits. Despite having a relatively high RPFR (Table 5), the sample analyzed in this study has a very light $\delta^{11}B$ value ($-25‰$) that suggests it is a secondary mineral formed from the breakdown of primary borates with significant loss of boron from the system.

Overall, the boron isotope systematics of the minor borate minerals from the Turkish borate deposits can be used to infer the nature of the reactions involved during formation of the minor borate minerals. The presence of very light $\delta^{11}B$ values in the terrugite and the pandermite and howlite from Sultançayir provides clear evidence that these are secondary minerals in these instances and that there was substantial loss of boron from the system during their formation. However, in several cases the $\delta^{11}B$ values of the primary and secondary borate minerals are relatively close to those predicted by their respective RPFR values (e.g., in the howlite from Bigadiç), which indicates that little or no boron was lost during alteration. In other cases the $\delta^{11}B$ data are consistent with some of the minor borates being primary precipitates from the brine (e.g., meyerhofferite and inyoite from Bigadiç) and, hence, may give information concerning the evolution of conditions during formation of the deposits (e.g., water activity).

## 6. CONCLUSIONS

The boron isotope composition of 80 samples of borate minerals from the western Turkish deposit ranges from $-1.6$ to $-25.3‰$. The $\delta^{11}B$ values of the major ore-forming minerals (borax, ulexite, and colemanite) are dependent primarily on their mineralogy, with variations in the pH of the brine being of secondary importance. There is evidence to suggest a systematic variation in the source of boron to the deposits, with Emet having a greater contribution of boron from aluminosilicates and Bigadiç having a higher proportion of boron derived from limestones, while Kirka occupies an intermediate position.

The $\delta^{11}B$ values of the minor borates (veatchite-A, tunellite, kernite, terrugite, probertite, meyerhofferite, inderite, inyoite, hydroboracite, howlite, and pandermite) are also dependent on their mineralogy, but their $\delta^{11}B$ values can also provide information concerning the processes operating during their formation, i.e., whether they were primary precipitates or whether they are secondary minerals formed from the alteration of primary borates. In the latter case, the $\delta^{11}B$ data also provide information concerning the extent of boron loss form the system during their formation.

*Acknowledgments*—We are grateful to two anonymous reviewers for their helpful comments on an earlier version of this manuscript. This work was supported by a NATO grant to M.R.P. and C.H. and by Royal Society grants to M.R.P. We are especially grateful to Etibank and the mine managers and geologists for their generosity during fieldwork in Turkey.

## REFERENCES


Aggarwal J. K. and Palmer M. R. (1994) Boron isotope studies of natural materials: A review of analytical methods. *Analyst* **120,** 1301–1307.

Alonso R. N., Helvaci C., Sureda R. J., and Viramonte J.G. (1988) A new Tertiary borax deposit in the Andes. *Mineral. Deposita* **19,** 299–305.

Anovitz L. M. and Hemmingway B. S. (1996) Thermodynamics of boron minerals: Summary of structural, volumetric and thermochemical data. *Rev. Mineral.* **33,** 181–262.

Bowser C. J. (1965) Geochemistry and petrology of the sodium borates in the nonmarine evaporite environment. Ph.D. thesis, Univ. California.

Christ C. L., Truesdell A. H., and Erd R. C. (1967) Borate mineral assemblages in the system $Na_2O$-CaO-MgO-$B_2O_3$-$H_2O$. *Geochim. Cosmochim. Acta* **31,** 313–337.

Countryman R. L. (1977) The subsurface geology, structure and mineralogy of the Billie borate deposit, Death Valley, California. M.Sc. Thesis, Univ. California.

DePaolo D. J. and Ingram B. L. (1985) High-resolution stratigraphy with strontium isotopes. *Science* **227,** 938–941.

Griffen D. T. (1988) Howlite, $Ca_2SiB_5O_9(OH)_5$: Structure refinement and hydrogen bonding. *Amer. Mineral.* **73,** 1138–1144.

Helvaci C. (1977) Geology, mineralogy and geochemistry of the borate deposits and associated rocks of the Emet Valley, Turkey. Ph.D. thesis, Univ. of Nottingham.

Helvaci C. (1978) A review of the mineralogy of the Turkish borate deposits. *Mercian Geology* **6,** 257–270.

Helvaci C. (1983) Mineralogy of the Turkish borate deposits. *Jeoloji Mühendisligi* **17,** 37–54.

Helvaci C. (1984) Occurrence of rare borate minerals: Veatchite-A, tunellite, terruggite and cahnite in the Emet borate deposits, Turkey. *Mineral. Deposita* **19,** 217–226.

Helvaci C. (1994) Mineral assemblages and formation of the Kestelek and Sultançayir borate deposits. *Proc. 29th Intl. Geol. Congr. Part A,* 245–264.

Helvaci C. (1995) Stratigraphy, mineralogy and genesis of the Bigadiç borate deposits, Western Turkey. *Econ. Geol.* **90,** 1237–1260.

Helvaci C. and Firman R. J. (1976) Geological setting and mineralogy of Emet borate deposits, Turkey. *Trans. Sect. B Inst. Mining Metal.* **85,** B142–B152.

Inan K. (1973) The mineralogy and geochemistry of the Kirka borate deposit Turkey. Ph.D. Thesis, Univ. Manchester.

Inan K., Dunham A. C., and Esson J. (1973) Mineralogy, chemistry and origin of Kirka borate deposit, Eskisehir Province, Turkey. *Trans. Inst. Mining Metal.* **82B,** 114–123.

Ishikawa T. and Nakamura E. (1993) Boron isotope systematics of marine sediments. *Earth Planet. Sci. Lett.* **117,** 567–580.

Kakihana H., Kotaka M., Satoh S., Nomura M., and Okamoto M. (1977) Fundamental studies on the ion-exchange separation of boron isotopes. *Bull. Chem. Soc. Japan* **50,** 158–163.

Kistler R. B. and Helvaci C. (1994) Boron and borates. In *Industrial Minerals and Rocks,* 6th ed. (ed. D. D. Carr), pp. 171–186. Society of Mining, Metallurgy and Exploration, Inc.

Oi T., Nomura M., Musashi M., Ossaka T., Okamoto M., and Kakihana H. (1989) Boron isotopic composition of some boron minerals. *Geochim. Cosmochim. Acta* **53,** 3189–3195.

Palmer M. R. (1996) Boron isotope geochemistry: An overview. *Rev. Mineral.* **33,** 709–744.

Palmer M. R. and Helvaci C. (1995) The boron isotope geochemistry of the Kirka borate deposit, western Turkey. *Geochim. Cosmochim. Acta* **59,** 3599–3605.

Palmer M. R. and Slack J. F. (1989) Boron isotopic composition of tourmaline from massive sulfide deposits and tourmalinites. *Contrib. Mineral. Petrol.* **103,** 434–451.

Palmer M. R., London D., Morgan G. B., and Babb H. A. (1992) Experimental determination of fractionation of $^{11}B/^{10}B$ between tourmaline and aqueous vapor: A temperature- and pressure-dependent reaction. *Chem. Geol.* **101,** 123–129.

Peng Q. M. and Palmer M. R. (1995) The Palaeoproterozoic boron deposits in eastern Liaoning, China: A metamorphosed evaporite. *Precambr. Res.* **72,** 185–197.

Slack J. F., Palmer M. R., and Stevens B. P. J. (1989) Boron isotope evidence for the involvement of nonmarine evaporites in the origin of the Broken Hill ore deposits. *Nature* **342,** 913–916.

Smoot J .P. and Lowenstein T. K. (1991) Depositional environments of nonmarine evaporites. In *Evaporites, Petroleum and Mineral Resources* (ed. J. L. Melvin); *Developments in Sedimentology* **50,** 189–348.

Spivack A. J. and Edmond J. M. (1986) Determination of boron isotopes by therma ionization mass spectrometry of the dicesium metaborate cation. *Anal. Chem.* **58,** 31–35.

Sunder M. S. (1980) Geochemistry of the Sarikaya borate deposits (Kirka-Eskisehir). *Bull. Geol. Congress Turkey* **2,** 19–34.

Appendix A. Kirka deposit

| Sample | Mineralogy | Description |
|---|---|---|
| CH-5 | pandermite | massive nodule from ulexite-colemanite transition zone |
| CH-7 | ulexite | fibrous silky layer of ulexite from below borax zone |
| CH-8 | borax | massive borax from lower part of borax zone |
| CH-9 | ulexite | fibrous layer of primary ulexite from above the borax zone |
| CH-10 | ulexite | powdery ulexite within cavities in upper part of borax zone, possibly secondary after dissolution of borax |
| | inderite | large (1 cm) crystals in cavities |
| CH-11 | kernite | very rare mineral from central part of borax zone |
| CH-12 | ulexite | 1cm thick layer of ulexite from above the borax zone |
| CH-14 | borax | massive borax from middle of borax zone |
| CH-15 | borax | bedded borax from middle of borax zone |
| CH-16 | colemanite | radiating colemanite nodule 2cm in diameter from top of deposit |
| CH-17 | colemanite ulexite | white nodular ulexite growing on radiating crystals of colemanite from just above borax zone |
| CH-18 | ulexite borax | small (5cm) nodules of ulexite on top of bedded borax from top of borax zone |
| CH-22 | colemanite | small (3cm) colemanite nodule from small Göçenoluk deposit northwest of main deposit, thought to correlate with colemanite in main deposit below borax zone |
| CH-24 | borax | large (10cm thick) vein of borax cross cutting main borax zone, probably secondary replacement of orginal borax |
| CH-57 | tunellite | clear large (0.5 cm) crystals from upper ulexite-colemanite transition zone |
| MRP-4 | borax | bedded borax from main borax zone |
| MRP-5 | borax | thick (15cm) vein of clear borax cross cutting main borax zone, probably formed from recrystallisation of bedded borax |
| MRP-11 | ulexite | small (5cm) discoidal nodule of ulexite with fine grained ulexite infilling septarian cracks, from just above main borax zone |
| MRP-12 | colemanite | large (30cm) nodule of radiating colemanite with cross cutting veins of recrystallised colemanite and fine grain primary colemanite filling septarian cracks, from above main borax zone |
| MRP-14 | colemanite | large (25cm) nodule of radiating colemanite from above main borax zone |
| MRP-17 | ulexite | 1cm thick layer of ulexite from above the borax zone |

Appendix B. Bigadiç deposit

| Sample | Mineralogy | Description |
|---|---|---|
| Simav | | |
| CH-1 | colemanite | large (15 cm) rosette of clear crystals |
| CH-2 | pandermite | massive, chalky fine-grained white nodule |
| CH-25 | colemanite<br>ulexite | radiating colemanite rosette covered with powdery layer of ulexite |
| CH-43 | colemanite | large (10 cm) rosette of clear crystals |
| CH-49 | colemanite | large (10 cm) rosette of clear crystals |
| CH-52 | meyerhofferite | relative fine-grained nodular form |
| CH-53 | ulexite | thin bed within main colemanite band |
| MRP-44 | meyerhofferite<br>colemanite | intergrowth of fine grained crystals of both minerals in nodule |
| MRP-48 | colemanite | large (10 cm) rosette of clear crystals |
| Acep | | |
| CH-13 | colemanite | fine grained nodule |
| CH-21 | inyoite | very rare mineral, large (1 cm) crystals |
| MRP-40 | colemanite | discoidal nodule of fine grained crystals overgrown by coarser grains |
| MRP-47 | inyoite<br>colemanite<br>ulexite | silky white rosettes of ulexite intergrown with fibrous rosette of colemanite with overgrowth of large (1 cm) inyoite crystals |
| Kireçlik | | |
| CH-44 | colemanite | massive clear colemanite crystals |
| CH-51 | colemanite | pea-sized clay-rich nodules in clay layer |
| CH-54 | ulexite | silky, fibrous nodule |
| Kurtpinari | | |
| CH-3 | ulexite | white, fibrous nodule |
| CH-46 | colemanite | 1 cm thick layer of massive colemanite in clay layer |
| CH-50 | howlite | 1 cm nodules in same clay layer as sample CH-46 |
| On Günevi | | |
| CH-45 | ulexite | fibrous crystals in nodule |
| Tülü | | |
| CH-4 | colemanite | 2–3 cm sized rosettes |
| CH-47 | colemanite | 2–3 cm sized rosettes |
| CH-48 | colemanite | 3 cm sized nodules in clay matrix |
| MRP-34 | colemanite | radiating crystals in 3–4 cm rosette |
| MRP-36 | pandermite | massive white nodule with black (organic?) veins |

Appendix C. Kestelek deposit

| Sample | Mineralogy | Description |
|---|---|---|
| CH-19 | colemanite | disk-shaped nodules with high clay content |
| CH-36 | colemanite | large (3–4 cm) diagenetic crystals |
| CH-37 | ulexite | fan-shaped fibrous crystals |
| CH-38 | probertite | large (10–15 cm long) fibrous crystals |
| CH-39 | hydroboracite | radiating fibrous needles 3 cm long |

Appendix D. Sultançayir deposit

| Sample | Mineralogy | Description |
|---|---|---|
| CH-20 | pandermite | 1 cm sized nodules in clay matrix within gypsum lens |
| CH-90 | pandermite + colemanite | powdery white pandermite in interstices of 1 cm sized radiating colemanite nodules |
| CH-91 | howlite | 3 cm sized massive nodule |
| CH-92 | howlite | 5 cm sized massive nodule |

Appendix E: Emet deposit

| Sample | Mineralogy | Description |
|---|---|---|
| Killik | | |
| CH-23 | colemanite | large (20 cm), clay-rich nodule with some As mineralization |
| CH-27 | hydroboracite | large (3–4 cm) fibrous, radiating crystals with some As mineralization |
| CH-28 | veatchite-A | coliform nodules, probably replacing colemanite |
| Espey | | |
| CH-26 | colemanite | dark-coloured large (5–8 cm) radiating colemanite crystals surrounded by mantle of light coloured colemanite |
| CH-32 | hydroboracite | large (3–4 cm), vugh-rich, radiating crystals, with large amounts of As mineralization |
| MRP-18 | colemanite | dark-coloured large (5–8 cm) radiating colemanite crystals |
| MRP-21 | colemanite | dark-coloured large (5–8 cm) radiating colemanite crystals surrounded by mantle of light coloured colemanite |
| MRP-23 | hydroboracite | large (3–4 cm), vugh-rich, radiating crystals, with large amounts of As mineralization |
| Göktepe | | |
| CH-33 | colemanite | weathered, clay-rich sample |
| Dereköy | | |
| CH-30 | colemanite | large (3–4 cm) crystals coexisting with celestine |
| Hisarcik | | |
| CH-6 | colemanite | small, radiating rosettes |
| CH-29 | colemanite | large, clay-rich, radiating, fibrous crystals with some As mineralization |
| CH-34 | colemanite | large radiating fibrous nodule, coexisting with orpiment and realgar |
| CH-42 | colemanite | dark, fine-grained nodule |
| CH-56 | terrugite | coliform nodule that appears to be replacing colemanite |